Springer Series in Materials Science 125

High-Temperature Superconductors

Bearbeitet von
Ajay Kumar Saxena

1. Auflage 2012. Taschenbuch. xiv, 224 S. Paperback
ISBN 978 3 642 26102 2
Format (B x L): 15,5 x 23,5 cm
Gewicht: 373 g

2

Crystal Structure of High Temperature Superconductors

2.1 Introduction

It has been shown by several groups of scientists including Hazen et al. [1] that the new high temperature superconductors (HTSCs) are structurally flawed members of a crystallographic family known as perovskites.

2.1.1 Perovskite Structure

Perovskites are ceramics (solid materials combining metallic elements with non-metals, usually oxygen) that have a particular atomic arrangement. In their ideal form, described by generalised formula ABX_3, they consist of cubes made up of three distinct chemical elements (A, B and X) that are present in a ratio 1:1:3. The A and B atoms are metallic cations (positive) and X atoms are non-metallic anions (negative). An A cation – the largest of the two kinds of metals – lies at the centre of each cube, the B cations occupy all the eight corners and the X anions lie at the mid-points of cube's twelve edges (Fig. 2.1).

2.2 The Structure of $YBa_2Cu_3O_{7-x}$

The compound $YBa_2Cu_3O_7$ is superconducting ($T_c = 90\,K$) and has orthorhombic symmetry and, the structure has two Cu–O sheets in the ab plane and Cu–O chains along the b-axis. The structure can be described as a perovskite with an oxygen deficit. In Fig. 2.1, B is the metallic cation Cu (small radius), surrounded by six oxygen ions occupying site X. The metallic cation site A is occupied by yttrium (large radius than B). By eliminating oxygen atoms from the ideal perovskite lattice, we obtain $YBa_2Cu_3O_7$ (Fig. 2.2a). Its unit cell contains.

- A layer of Cu–O having copper (Cu 1) surrounded by four oxygen ions
- A layer of BaO

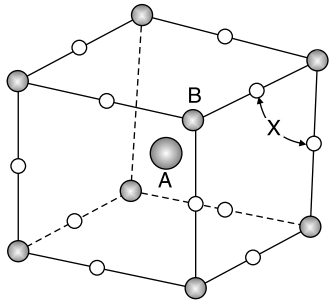

Fig. 2.1. The perovskite structure ABX_3

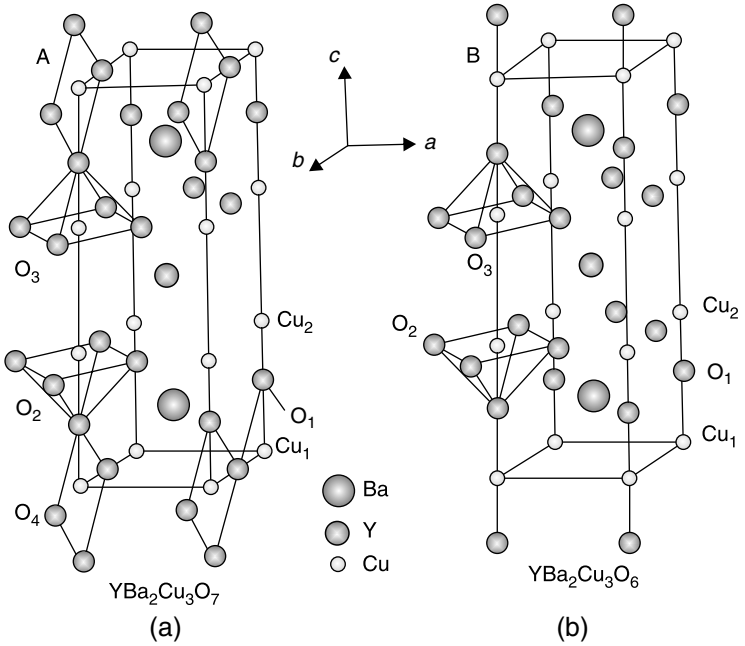

Fig. 2.2. The structure of YBCO **(a)** orthorhombic structure ($a_0 = 3.823$ Å, $b_0 = 3.885$ Å, $c_0 = 11.7$ Å) **(b)** tetragonal structure ($a_0 = b_0 = 3.86$ Å, $c_0 = 11.7$ Å)

- A layer of Cu–O, where (Cu 2) is surrounded by five oxygen ions forming a polyhedron
- A layer of yttrium, short of four oxygen

Thus, the stacking sequence of the (ab) planes is Y–CuO–BaO–CuO_2–BaO–CuO_2–Y (we will see in this chapter 5-that the configuration of copper–oxygen planes is Cu–O_2). It is to be noted that there are Cu–O chains along the b-axis. The presence of oxygen atoms in these chains are essential for superconductivity.

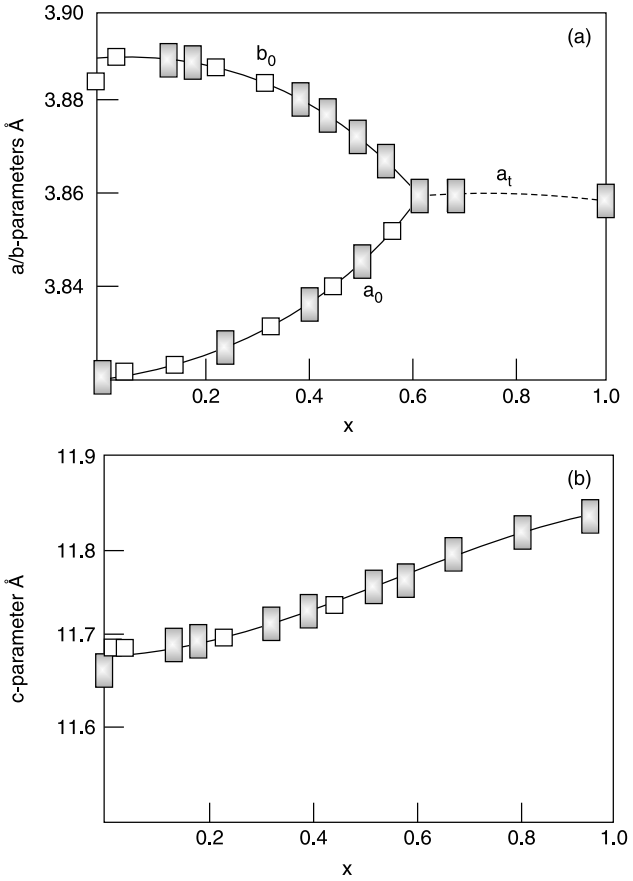

Fig. 2.3. Variation of the unit cell parameters of $Y_1Ba_2Cu_3O_{7-x}$ with the oxygen stoichiometry x. The oxygen deficiency leads to departure from orthorhombicity $\left(\frac{b-a}{b+a}\right)$

The general formula of the compound is $Y_1Ba_2Cu_3O_{7-x}$ where $0 \leq x \leq 1$. The lattice parameters vary with the oxygen content (x-value) and for $x \geq 0.6$, the structure is tetragonal. In $Y_1Ba_2Cu_3O_6$ ($x = 1$), there are no chain (O4 sites) oxygen and Cu in b-axis is in the 1^+ state. (Non-superconducting state). Thus, the unit cell parameters vary with the value of x in $Y_1Ba_2Cu_3O_{7-x}$ (i.e. a, b and c parameters vary with the oxygen-stoichiometry). This has been depicted in Fig. 2.3. The structure is orthorhombic for $x = 0$.

2.2.1 Variation of T_c with Oxygen Stoichiometry

The critical temperature T_c of $Y_1Ba_2Cu_3O_{7-x}$ also varies with x-value and the material becomes non-superconducting at $x \cong 0.6$ (Fig. 2.5).

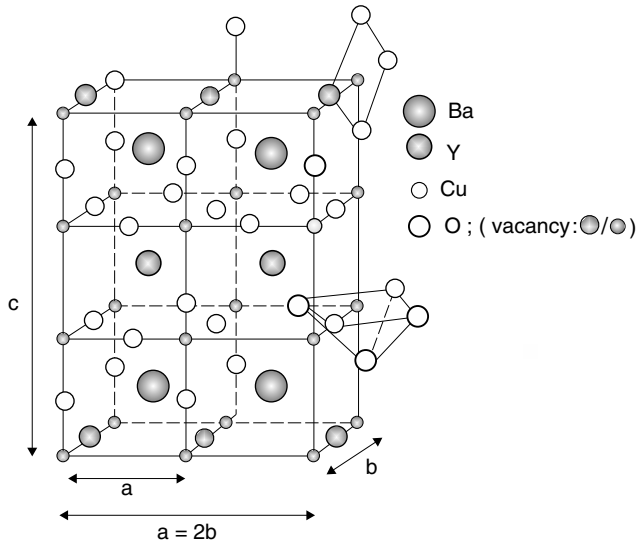

Fig. 2.4. Crystal structure with oxygen (⊕) disappearing from alternate chains in $YBa_2Cu_3O_{6.5}$ and complete disappearance of oxygen (⊖) from $YBa_2Cu_3O_{7-x}$ to give $YBa_2Cu_3O_6$ (It has been shown using neutron diffraction techniques and high resolution electron microscopy that the oxygen deficit is situated in the CuO_4 square plane layers and not in the CuO_5 pyramids). Every $1/x^{\text{th}}$ chain oxygen is missing for $YBa_2Cu_3O_{7-x}$

The T_c remains around 90 K from $x = 0$ to $x \approx 0.2$ (for $x = 0.25$, there are alternately "full" and half oxygen chains) and then shows a plateau at 60 K when $x = 0.3$–0.4. T_c is 45 K, when $x = 0.5$. Structural studies have revealed that oxygen vacancies may be ordered when $x = 0.5$ and 0.75 and no clear oxygen vacancy ordering has been found in the $x = 0.3$–0.4 range, (i.e. in the plateau region). For $x = 0.5$ (i.e. $YBa_2Cu_3O_{6.5}$), fully oxygenated Cu–O chains (as in $YBa_2Cu_3O_7$) are present along b-axis, alternating with fully vacant O4 sites (as in $YBa_2Cu_3O_6$) (see Fig. 2.4).

Thus, for $x = 1.0$, there are no chain oxygen atoms and T_c is zero. The value of x in a particular sample depends on the processing conditions, especially temperature and oxygen partial pressure. Even though x itself is temperature and atmosphere dependent, under equilibrium conditions at high temperatures, the transition appears always to occur at $x = 6.5$.

Figure 2.6 shows the cell-parameters for the orthorhombic structure of Y–Ba–Cu–O. The double CuO_2 layers are a feature common to all the HTSCs and are believed to be the key to the occurrence of high temperature superconductivity in these oxides.

The anisotropic structure of these compounds is reflected in the anisotropy of the relevant intrinsic electronic properties of these materials, as shown in Table 2.1.

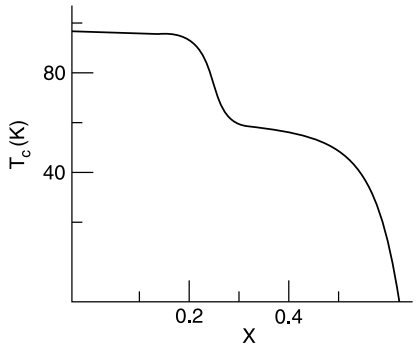

Fig. 2.5. Variation of the superconducting transition temperature T_c of $YBa_2Cu_3O_{7-x}$ with the oxygen stoichiometry x

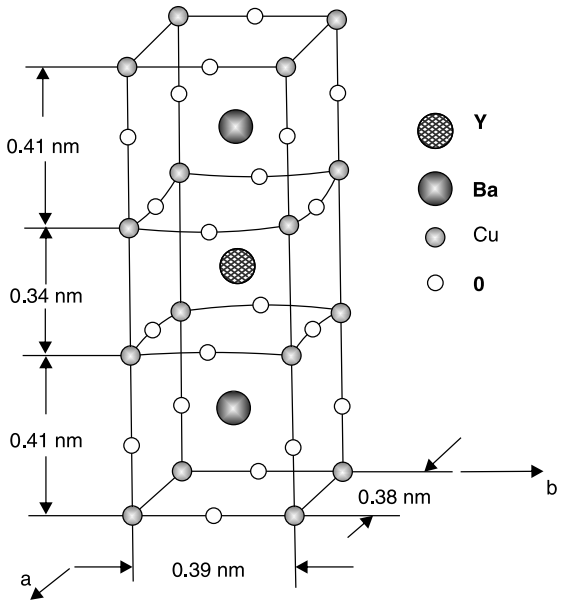

Fig. 2.6. The orthorhombic (distorted) crystal structure of YBCO superconductor

Table 2.1. Relevant intrinsic properties of YBa_2–Cu_3O_{7-x}

	Parallel to *c*-axis	Parallel to *ab*-plane
ξ(Å)	∼2 to 3	∼15 to 20
λ(Å)	1,500	7,500
J_C(Acm^{-2} at 77 K)	10^4	10^6
H_{c2}	150 T	30 T

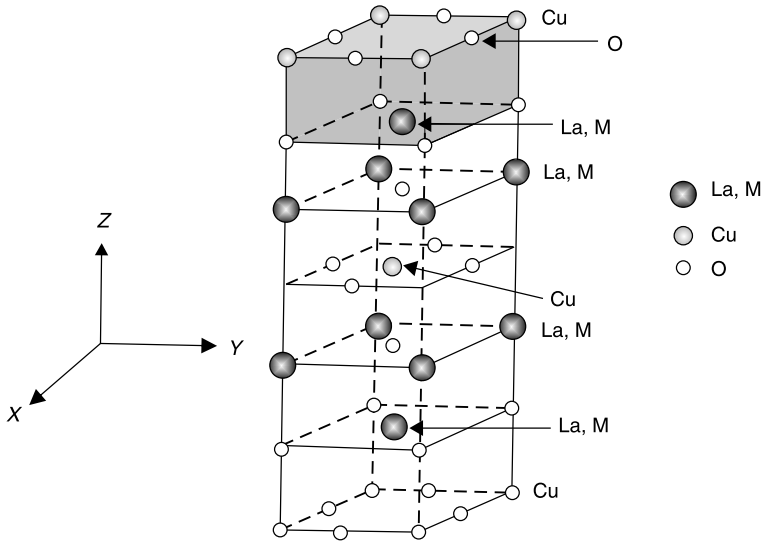

Fig. 2.7. The crystal structure of $La_{2-x}M_xCuO_4$ (M = Ba or Sr). For $x = 0$, $a = b = 3.77$ Å, $c = 13.25$ Å. M atoms occupy La site in La_2CuO_4

2.3 The Structure of $La_{2-x}M_xCuO_4$

Unlike YBCO (which have their structure derived from ideal perovskite by an ordered removal of oxygen atoms), La-, Bi-, or Tl-based cuprates have structures derived from ideal perovskite structure through an intergrowth phenomenon. Structure of $La_{2-x}M_xCuO_4$ is shown in Fig. 2.7.

M is the alkaline earth element (Sr or Ba). It can substituted on the La-site. $La_{1.85}Sr_{0.15}CuO_4$ has a tetragonal K_2NiF_4 type of layered perovskite structure. The structure can be viewed as a stacking of

$$–CuO_2–LaO–LaO–CuO_2–LaO–LaO–CuO_2–$$

$La_{2-x}M_xCuO_4$ shows the highest T_c around a critical value of x (0.15 for Sr and 0.2 for Ba with T_cs of 30 K and 35 K respectively).

2.4 The Structure of Bi-Based Cuprate Superconductors

The discovery of the high T_c superconductor $La_{2-x}(Ba/Sr)_xCuO_4$ with $T_c \sim 40$ K and $YBa_2Cu_3O_{7-x}$ with T_c of ~90 K led to an intensive search for new oxide superconductors of still higher T_cs (>100 K). No new superconductor with T_c higher than that of $YBa_2Cu_3O_{7-x}$ was reported upto January 1988. In May 1987, Michel et al. [2] reported the discovery of superconductivity between 7 and 22 K in rare-earth-less material Bi–Sr–Cu–O. Because of the intense interest in the 90 K material YBCO, at that time, their report did

not attract widespread interest. However, attention quickly focused on the Bi-containing cuprate superconductors in January 1988, when addition of Ca to the Bi–Sr–Cu–O ternary led Maeda et al. [3] to the discovery of bulk superconductivity at 85 K and evidence of superconductivity upto 110 K in the Bi–Sr–Ca–Cu–O system. The compound with formula $Bi_4Sr_3Ca_3Cu_4O_{16}$ was found to be responsible for superconductivity at 85 K in the Bi-system and its structure was established [4, 5].

The crystal substructure can be viewed as a three dimensional packing of $Bi_2Sr_2Ca_1Cu_2O_8$ slabs along the c-axis, with the main feature being the presence of the two Bi–O layers separated by 3.0 Å and shifted, with respect to each other (crystallographic shear) along the diagonal direction of the perovskite sub-cell. Tarascan et al. [6] showed the evidence that the 100 K phase has the Bi-2:2:2:3 formula and its structure contains three CuO_2 layers: The three phases of Bi–Sr–Ca–Cu–O can be represented by the general formula $Bi_2\ Sr_2Ca_{n-1}Cu_nO_y$ ($n = 1$, 2 and 3) and have a pseudo-tetragonal structure (Fig. 2.8), which can be described as a stacking of a basic $Bi_2Sr_2CuO_6$ unit with either zero, one or two $CaCuO_2$ slabs inserted. The c-lattice parameter increases from 24.6 to 30.6 Å and finally to 37.1 Å in going from $n = 1$ to $n = 2$ and $n = 3$, and the increase results from the progressive addition of 2×1 and 2×2 (doubled because of the crystallographic shear) $CaCuO_2$, each about 3 Å thick, to the stacking sequence in the unit cell.

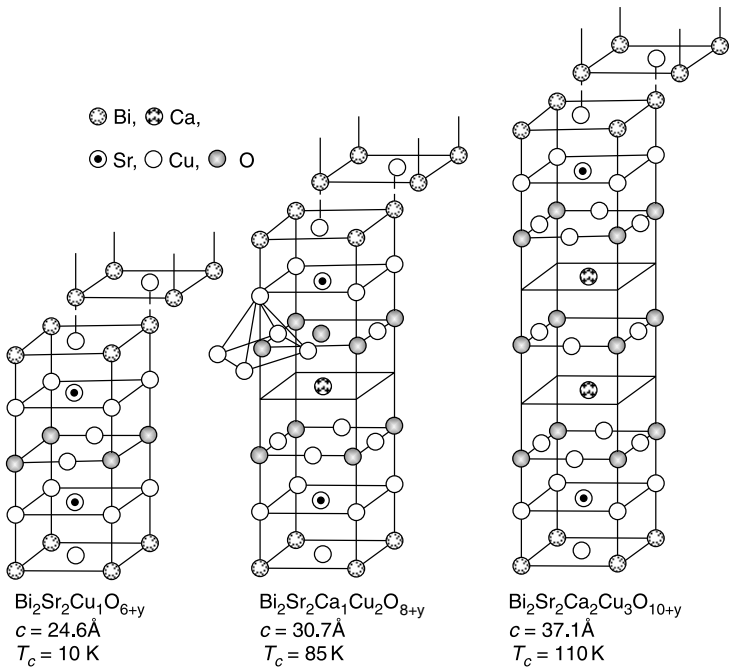

Fig. 2.8. The crystal structures of the Bi phases of general formula $Bi_2Sr_2Ca_{n-1}Cu_nO_y$ with $n = 1$, 2 and 3

For $Bi_2Sr_2Ca_1Cu_2O_8$, the stacking sequence is

Bi–Sr–Cu–Ca–Cu–Sr–Bi.

In $Bi_2Sr_2Ca_2Cu_3O_{10}$, the layer sequence is

Bi–Sr–Cu–Ca–Cu–Ca–Cu–Sr–Bi.

The Bi-based high T_c superconductors [$Bi_2Sr_2Ca_{n-1}Cu_nO_y$ for$n = 2$ and 3] are superior to the YBCO in respect of higher T_c. This class of superconductors (unlike YBCO) are resistant to water or humid atmosphere and have the advantage of compositional/oxygen stability, e.g. some of its superconducting phases do not gain or lose oxygen, when the material is annealed at ∼850°C. Another advantage of the BSCCO materials relates to the fact that BiO layers being Vander Waal bonded, this material can be easily rolled. This property has been utilised successfully for tape-casting and its texturing.

2.5 Structure of Thallium-Based Cuprate Superconductors

The discovery of 30 K superconductivity in the La–Ba–Cu–O system stimulated a worldwide search for even higher T_c superconductors. Elemental substitutions proved to be most effective in raising the transition temperature. Substitution of Sr for Ba produced 40 K superconductivity in the La–Ba–Cu–O system and substitutions of Y for La produced the high T_c (∼90 K) superconductor Y–Ba–Cu–O, and it became clear immediately that substitutions of other rare-earths for Y would produce superconductors.

Two approaches for rare-earth substitution were taken. One approach was the choice of the rare-earth with small or no magnetic moment, such as Lu and Yb, as a small concentration of magnetic ions is known to depress significantly, or even to destroy superconductivity in conventional superconductors. Another approach was the choice of the rare-earths with ionic radius close to that of Y, such as Gd and Ho, inspite of their large magnetic moment. After all the rare-earths were substituted, it was concluded that

(1) Substitution of magnetic rare-earths for Y in $Y_1Ba_2Cu_3O_{7-x}$ did not influence significantly the transition temperature
(2) Ionic radius of rare-earths was important to superconductive behaviour of the (RE) $Ba_2Cu_3O_{7-x}$ compounds, e.g. substitution of La (the rare-earth with largest ionic radius) for Y produced superconductor with a relatively low transition temperature, usually below liquid nitrogen temperature, and the Lu-containing superconductor (Lu is the rare earth with smallest ionic radius) was difficult to be prepared in single phase, and
(3) The valence of the substituted rare earth was crucial to the superconductivity of (RE) $Ba_2Cu_3O_{7-x}$ compounds (Ce, Pr and Tb with both 3^+ and 4^+ valences did not form superconducting compounds)

The above mentioned facts strongly suggest that the valence and radius of rare-earth ions are more vital to the formation of rare-earth containing superconductors than the local magnetic effects.

Logically one would expect that other elements with 3^+ valence and similar ionic radius could also form similar superconducting compounds. Sheng and Hermann (University of Arkansas, Fayetteville) inspected the periodic table that the elements in Group IIIA were also characterised by a 3^+ valence and in particular Tl (thallium), the heaviest one in Gr IIIA, had an ionic radius (in 3^+ valence state) of 0.95 Å, similar to those of rare-earths (0.85–1.016 Å) and same as that of Eu^{3+}. These considerations motivated them to completely replace rare-earths in the (RE)–Ba–Cu–O system with thallium. Thus, the superconductivity in the Tl–Ba–Cu–O system was observed for the first time in October 1987 by Sheng and Hermann. Their samples contained no Ca, their nominal compositions were $Tl_2Ba_2Cu_3O_{8+x}$ and $TlBaCu_3O_{5.5+x}$. The sample consisted of many components and showed zero resistance above 80 K [7]. Soon after this, they added Ca to their samples and discovered superconductivity above 100 K in Tl–Ba–Ca–Cu–O system [8]. Their sample consisted of many chemical components. The superconducting phases were identified in Sheng and Hermann's sample by Hazen et al. [9]: $TlBa_2CaCu_2O_8$ and $Tl_2Ba_2Ca_2Cu_3O_{10}$. Then, Parkin et al. [10] changed the processing conditions to greatly increase the amount of $Tl_2Ba_2Ca_2Cu_3O_{10}$ phase and produced a material with bulk superconductivity at 125 K.

Ten perovskite-related oxides have been identified in Tl–Ba–Ca–Cu–O system. These are $Tl_1Ba_2Cu_1O_5$, $Tl_1Ba_2Ca_1Cu_2O_7$, $TlBa_2Ca_2Cu_3O_9$, $Tl_1Ba_2Ca_3Cu_4O_{11}$, $Tl_1Ba_2Ca_4Cu_5O_{13}$, $Tl_1Ba_2Ca_5Cu_6O_{15}$, $Tl_2Ba_2Cu_1O_6$, $Tl_2Ba_2CaCu_2O_8$, $Tl_2Ba_2Ca_2Cu_3O_{10}$ and $Tl_2Ba_2Ca_3Cu_4O_{12}$. For brevity, these phases are referred to as Tl:1201, Tl:1212, Tl:1223, Tl:1234, Tl:1245, Tl:1256, Tl:2201, Tl:2212, Tl:2223 and Tl:2234. The crystal structures of these phases, which form the homologous series are represented by general formula:

$$Tl_mBa_2Ca_{n-1}Cu_nO_{2(n+1)+m}$$
$$(m = 1, 2 \text{ and } n = 1 - 6)$$

as shown in Figs. 2.9 and 2.10.

All of these oxide have a tetragonal structure at room temperature. The oxides with Tl–O mono-layers have primitive tetragonal cells, whereas the oxides with Tl–O bilayers have body-centered tetragonal cells.

2.5.1 Comparison of Bismuth and Thallium Based Cuprates

Bismuth cuprates

(1) Are orthorhombic
(2) Show modulation in *ab* plane (with 4*b* periodicity)
(3) Possibility of intergrowth of members (of the series) at the unit cell level

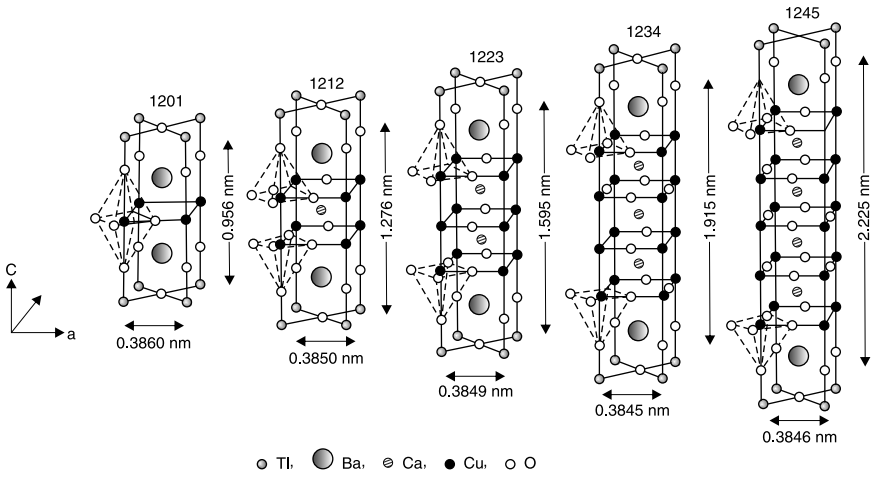

Fig. 2.9. Crystal structures of Tl monolayer superconducting oxides $TlBa_2Ca_{n-1}Cu_n\ O_{2n+3}\ (n = 1 - 5)$

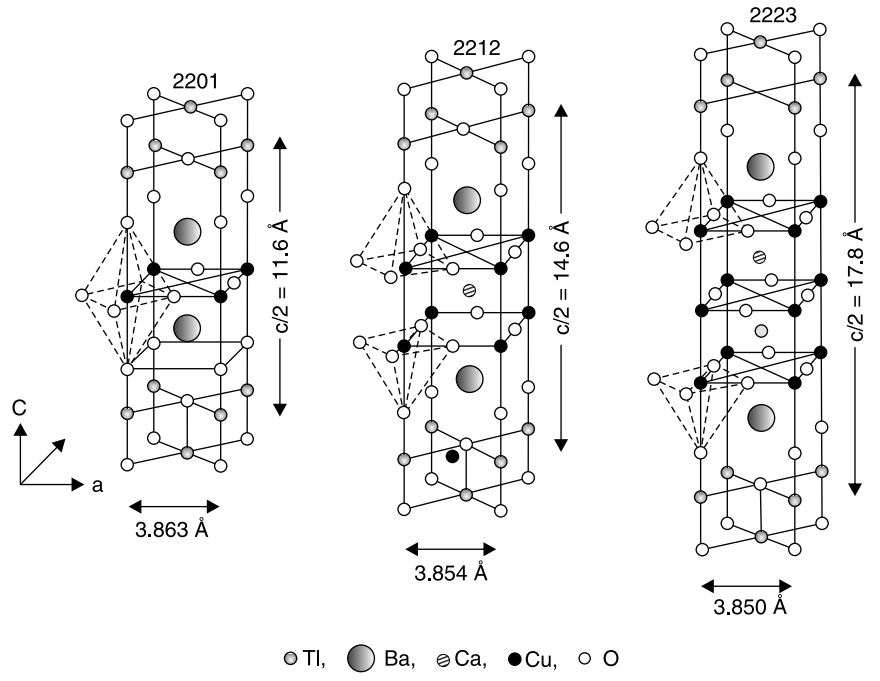

Fig. 2.10. Structure model of $Tl_2Ba_2Ca_{n-1}Cu_n\ O_{2n+4} (n = 1 - 3)$

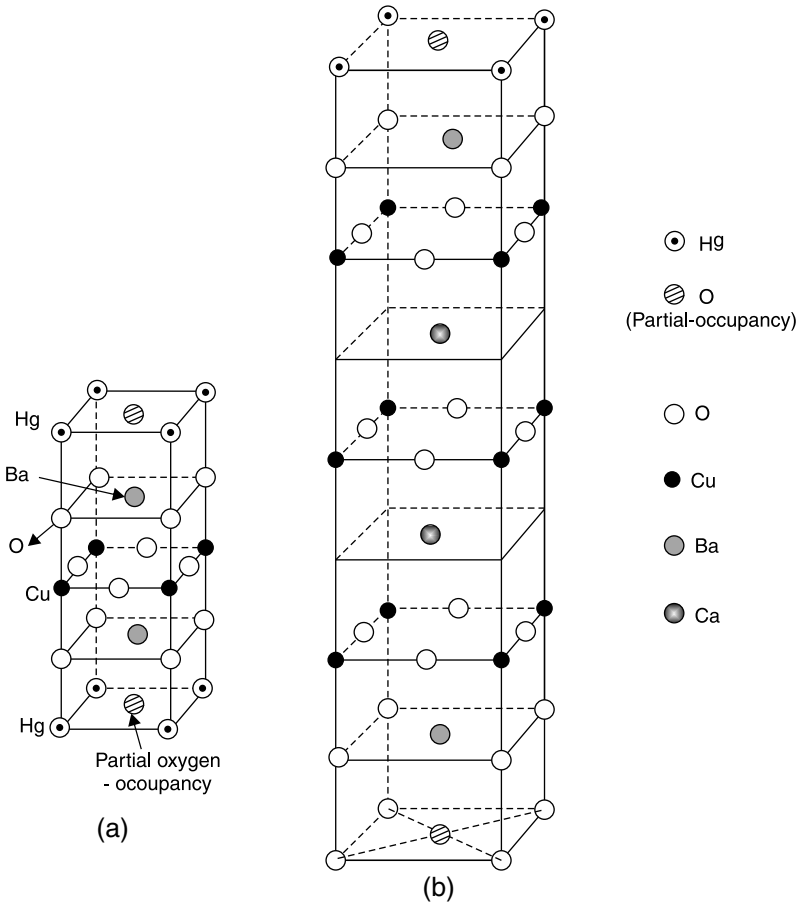

Fig. 2.11. Showing atom cluster model for central cell of (**a**) Hg-1201 and (**b**) Hg-1223 superconductors

Here, modulation is related to the oxygen content and structure of the Bi–O layers. There is never phasic purity because of (3).

In thallium cuprates, the phasic inhomogeneity is due to the co-occurrence (or intergrowth) of the different members of the series. Absence of twins is definitely established in these cuprates.

2.6 Mercury Based Cuprate Superconductors

Mercury bearing compound $HgBa_2RCu_2O_{6+\delta}$ (Hg:1212), where R is a rare-earth element, was synthesised by Putilin et al. [11]. It has a structure similar to the thallium bearing superconductor $TlBa_2CaCu_2O_7$ (Tl-1212), which has one TlO layer and two CuO_2 layers per unit cell and $T_c \sim 85\,K$ [12].

But inspite of the resemblance to Tl:1212, Hg:1212 was found to be non-superconducting. In 1993, Putilin et al. [13] reported the synthesis of the compound $HgBa_2CuO_{4+\delta}$ (Hg:1201) with only one CuO_2 layer per unit cell. It was found to be superconducting below 94 K. Its structure is similar to that of Tl:1201 ($T_c \leq 10$ K), but its T_c is considerably higher. The availability of such a material with high T_c and a single metal-oxide (HgO) layer may be important for technological applications, because a smaller spacing between CuO_2 planes leads to better superconducting properties in a magnetic field.

The structural arrangement of $HgBa_2CuO_{4+\delta}$ is similar to that of Tl Ba_2CuO_5, except for the oxygen stoichiometry of the HgO_δ and $TlO_{1-\delta}$ layers, respectively. For the former, δ is very small and for the latter, the $TlO_{1-\delta}$ layer is only slightly oxygen depleted. These different requirements for attaining the optimal concentration of holes (carriers) are due to the different preferred coordination geometries of the Tl^{3+} and Hg^{2+} cations. The rare-earth based Hg:1212 compounds were not found to be superconducting because the hole concentration in these phases might not be high enough for inducing superconductivity. Putilin et al. [14] replaced the trivalent rare-earth cation by divalent Ca^{2+} and obtained a superconductive transition temperature of above 120 K in Hg $Ba_2CaCu_2O_{6+\delta}$.

In 1993, Schilling et al. [15] reported their discovery of superconductivity above 130 K in a material containing $HgBa_2Ca_2Cu_3O_{8+\delta}$ (with three CuO_2 layers per unit cell) and $HgBa_2CaCu_3O_{6+\delta}$ (with two CuO_2 layers per unit cell) and an ordered superstructure comprising a defined sequence of the unit cells of these phases. A maximum transition temperature of ∼133 K had been obtained which was distinctly higher than the previously established value of 125–127 K observed in $Tl_2Ba_2Ca_2Cu_3O_{10}$.

In September 1993, a record T_c of ∼150 K in $HgBa_2Ca_2Cu_3O_{8+\delta}$ at quasi-hydrostatic pressure of 150 K-bar was obtained by Chu (Texas Centre for Superconductivity, U.S.A.). Such pressure effect on T_c might also be duplicated by chemical means, i.e. "chemical pressure" imposed by other "element" substituted on Hg-site (published in Nature) (Previous record of $T_c \sim 135$ K in Hg:1223 was at ambient pressure).

It has been found that electronic structure for $\delta = 0$ reveals that

1. Total density of states $N(E_F)$ per cell at E_F is 36 states Ryd^{-1} per cell. It is close to the value (40) for $Y_1Ba_2Cu_3O_{6+x}$. Also, it is much larger than 16 states Ryd^{-1} per cell for $La_{1.85}Sr_{0.15}CuO_4$ (Note: $N(E_F)$, is mainly from the Cu $3d_{x^2-y^2}$ and O$2p$ orbital in the CuO_2 layers.)
2. The two-dimensionality of the electronic structure of Hg:1223 is higher than that of $La_{1.85}Sr_{0.15}CuO_4$ (i.e. the carriers tend to move mainly in the CuO_2 layers).
3. The DOS curves of Ba and Ca are almost above the Fermi energy and, therefore, indicate that this stabilises the crystal structure and hence, Ba and Ca serve as electron-reservoirs.

It is to be noted that Hg:1201 is overdoped and only slightly excess oxygen (i.e. $\delta > 0$ and $\delta << 1$) introduces holes into the CuO_2 layers. In contrast to this, Cu atom oxidation state in Tl:1.201 is itself high (=+3).

2.7 Characteristics of High Temperature Superconductors

Some of the common characteristics of oxide high T_c cuprate superconductors are as follows:

(1) They have their structure derived from ideal perovskite structure (therefore, termed as defect perovskite structure), either through an intergrowth phenomenon or by an ordered removal of oxygen atoms.
(2) They have a layered crystal structure consisting of one or more CuO_2 layers. Each copper atom in a Cu–O_2 plane is strongly covalently bonded, in a nearly square-planar arrangement, with four oxygen atoms at a distance of 1.9 Å. (The Cu–O bond length).
(3) Copper is present in the mixed valence state involving a partial oxidation of Cu^{2+} to Cu^{3+}.
(4) There is a charge transfer, to and from the CuO_2 layers, which is induced by doping near the metal-insulator phase boundary (in the phase-diagram) existing in all oxide high T_c superconductors.
(5) The sign of Hall coefficient is positive, indicating that the charge carriers are holes in all oxide HTSCs, except $Nd_{2-x}Ce_xCuO_4$, which is an electron superconductor. Hall coefficient for a magnetic field H parallel to the ab plane is much smaller than for H parallel to the c-axis.
(6) When rare-earth (RE) ions replace Y in $YBa_2Cu_3O_7$, T_c remains virtually unchanged and most of the transport properties are unaffected. However, the specific heat data of (RE) $Ba_2Cu_3O_7$ compounds, which are within 2% of the $YBa_2Cu_3O_7$ for $T > T_c$ show drastic differences at low temperatures. This arises due to the magnetic interactions between the paramagnetic ions as well as between these ions and the crystal field. This establishes that superconductivity and magnetism can coexist in the RE compounds and the RE ions do not participate in superconductivity.
(7) The normal state transport properties are highly anisotropic. In YBCO, there is a linear dependence of the ab plane resistivity (ρ_{ab}). But the c-axis resistivity (ρ_c) shows a semiconducting dependence ($\propto 1/T$) for less oxygenated samples and $\rho_c \propto T$ for well oxygenated samples. $\rho_c/\rho_{ab} \sim 30$ at room temperature. Similar anisotropic behaviour is observed for other HTSCs.
(8) All of them are type II superconductors. The lower critical field H_{c1} and the upper critical field H_{c2} are highly anisotropic.

$$H''_{c2}(0) = 120\,\mathrm{T} \quad \text{and} \quad H^{\perp}_{c2}(0) = 510\,\mathrm{T} \quad \text{for} \quad YBa_2Cu_3O_7.$$

(9) The two fundamental superconductivity parameters viz. the coherence length ξ and the penetration depth λ are also highly anisotropic. ξ_{ab} = 20–30 Å and ξ_c = 2–3 Å for $YBa_2Cu_3O_7$, Further, the magnitude of coherence length is quite small as compared to that for conventional superconductors.

(10) There is near absence of isotope effect in high T_c superconductor.
(11) The value of $2\Delta(0)/(k_B T_c)$ is smaller for tunnelling of pairs perpendicular to the *ab*-plane (i.e. it is in the range of 3.8–4), while its value parallel to the plane is 5.8–6.0.
(12) The low temperature specific heat of HTSCs in the superconducting phase is due to three contributions:
   – $C = \alpha T^{-2} + \gamma T + \beta T^3$.
   – The first term gives a Schottky-like anomaly and arises from magnetic impurities. The second is a linear contribution similar to that for free electrons in a metal. The third is Debye contribution from the lattice. The absence of the exponential dependence of the electronic specific heat (expected on the basis of the BCS theory) is a major departure from the properties of the conventional superconductors. The linear term is now believed to arise from the presence of impurities.
(13) The phononic mechanism of superconductivity (The BCS theory) has certain limitations in theoretically explaining the mechanism of superconductivity in the cuprate high T_c superconductors. Various other mechanisms have been proposed (e.g. Anderson's RVB model, Schrieffer's spin-bag model, bipolaron model, etc.) but still, no suitable mechanism is able to explain satisfactorily various normal-state and superconducting properties of these materials.

2.7.1 Resemblance Between HTSC and Conventional Superconductors

The following are the points of resemblances:

1. Superconducting state is made up of paired carriers
2. Presence of a true energy gap ($\Delta(k) \neq 0$ for all values of k)
3. Jump in specific heat at $T = T_c$
4. The pair wave function has s-wave symmetry
5. Presence of a Fermi-surface

2.7.2 Unusual Properties of HTSCs

(1) Small coherence length ξ
   (This reduces the pinning energy implying weak pinning)
(2) Large penetration depth λ
   (This softens the flux line lattice (FLL))

(3) Large energy gap (Δ)
(4) Large anisotropy (cf. $\xi_{ab} > \xi_c$)
(This is due to layered structure)
(5) Small Fermi energy (E_{F})
(6) High T_c ($\sim$90 to 130 K)
(7) Smaller carrier concentration
(There are only $\leq$5 pairs per coherence volume as compared 10^4 pairs per coherence volume for BCS superconductor)
(8) High H_{c2} $\left(=\phi_0/2\pi\xi^2\right)$,
which is anisotropic and much larger when applied parallel to the planes than when applied perpendicular to the planes $\sim$1 M Gauss (for YBCO), which is 3–5 times the fields available presently
(9) Heat transport dominated by lattice

$$(k_{\mathrm{el}} << k_{\mathrm{lat}})$$

(10) The jump in heat capacity is not sharp
(11) (a) Sound velocity (elastic constants) is dramatically affected at T_{c} (unaffected for conventional superconductors)
(b) Presence of low-lying optical phonon modes
(12) The ratio $\frac{\Delta(0)}{E_{\mathrm{F}}}$, which indicates fraction of electrons paired, is much larger than in conventional superconductors

It may be mentioned here that in HTSCs, the existence of pairs is reflected experimentally by

1. ac Josephson effect
2. Direct measurement of ϕ_0 (flux quantum)

and

3. Little–Parks oscillations

2.8 Fermi Energy and Fermi Velocity of Superconductors

One of the most unusual fundamental properties of HTSCs is that one particle excitations are characterised by low values of Fermi-energy (E_{F}) and Fermi velocity v_{F} (see Table 2.4).

Table 2.4 shows effective mass m^*, Fermi wave vector k_{F}, Fermi velocity v_{F} and Fermi energy E_{F} for a conventional and high T_{c} superconductor.

The ratio $\Delta(0)/E_{\mathrm{F}} \sim \left(10^{-4}\right)$ for low T_{c} superconductors, where as it is $\sim(10^{-1})$ for high T_{c} materials.

The ratio $\Delta(0)/E_{\mathrm{F}}$ is an important superconducting parameter. It shows what faction of the electronic states are directly involved in pairing. The small value in ordinary superconductors means that only a small number of states near the Fermi-surface are involved in pairing. However, large value of

Table 2.2. Lattice parameters of Hg based superconductors

Cuprate	T_c^a(K)	Lattice parameters
Hg-1201	94	$a(=b) = 3.85$ Å, $c = 9.5$ Å
Hg-1212	120	$a(=b) = 3.85$ Å, $c = 12.6$ Å
Hg-1223	133	$a(=b) = 3.85$ Å, $c = 15.7$ Å

[a]At ambient pressure

Table 2.3. The comparison of estimated parameters for Hg-1223 and Y-123

Parameters	Hg-1223	Y-123
T_c	133 K	90 K
H_{c1}(o) along c-axis	290 Oe	1×10^4Oe
H_{c2}(o) along c-axis	190×10^4 Oe	120×10^4 Oe
$\lambda_{ab}(0)$	1,650 Å	1,300 Å
$\xi_{ab}(0)$	13 Å	10–15 Å
$\gamma(=\lambda_c/\lambda_{ab})$ (anisotropy parameter)	17	6
$2\Delta/k_BT_c$ (4.2 K)	4.2	6–8
$\Delta C_p/T_c^a$	27 mJ mole^{-1}K^{-2}	45–65 mJ mole^{-1}K^{-2}

[a]Size of discontinuity in electronic contribution to specific heat
(Note: The expected value for $\Delta C_p/T_c$ for 100% single phases of Hg-1223 is 45 mJ mole^{-1}K^{-2})

Table 2.4. Some physical parameters of La-Sr-Cu-O

Quantity	Conventional metals	$La_{1.8}Sr_{0.2}CuO_4$
m^*	(1–15) m_e	$5\,m_e$
k_F(cm^{-1})	10^8	3.5×10^7
v_F(cm s^{-1})	(1–2) $\times 10^8$	8×10^6
E_F(eV)	(5–10)	0.1

$\Delta(0)/E_F$ for cuprates corresponds to a significant faction of the carriers being paired up. Naturally, this implies a short coherence length.

Since in conventional superconductors $\frac{\Delta(0)}{E_F} << 1$, pairing can occur only near the Fermi surface (Cooper's theorem). Thus, the states on the Fermi surface form a two-dimensional system in momentum space. This is important because in 2D, any attraction will lead to the formation of a bound state (pairs). The possibility of having a large value of $\frac{\Delta(0)}{E_F}$ and a short ξ is directly related to the quasi-two-dimensional structure of the cuprates (layered structure). Quasi-two-dimensional carrier motion forms a favourable condition for pairing. Thus, this makes pairing possible, even for states that are distant from the Fermi surface (The *Fermi surface* is a locus in momentum space, where the occupation of the electronic states drops abruptly and where the energy required to create particle-hole excitations vanishes).

2.9 Comparison of High T_c Cuprates with Typical Metals in Relation to Normal State Resistivity

In the normal state (of HTSC cuprates), the in-plane resistivity ρ_{ab} increases with temperature (i.e. metallic behaviour) whereas ρ_c decreases with temperature. Thus, the system is metallic in ab-plane and non-metallic, perpendicular to it. (Extrapolated zero temperature value of ρ_{ab} is nearly zero in very clean samples). Resistivity in typical metals is due to

1. Scattering of electrons by lattice vibrations
2. Other electrons
3. Imperfections

None of these yields the observed temperature dependence for cuprate superconductors.

The linear temperature dependence in cuprates imply that inverse life-time (or decay rate) of a carrier is proportional to its excitation energy. Further, the normal state (i.e. above T_c), arising out of the motion of oxygen $2p$-holes in a background of magnetic copper d-holes (with which they mix), is poorly understood.

This family of materials cannot be considered as standard metals or as standard anti-ferromagnetic insulators.

The normal state properties of high T_c cuprates are anomalous, in the sense that they do not fit in with conventional Fermi-liquid[1] theory.

References

1. R.M. Hazen et al., Phys. Rev. **B35**, 7238 (1987)
2. C. Michel et al., Z. Phys. **B68**, 421 (1987)
3. H. Maeda et al., Jpn. J. Appl. Phys. **27**, L209 (1988)
4. J.M. Jarascan et al., Phys. Rev. **B37**, 9382 (1988)
5. S.A. Sunshine et al., Phys. Rev. **B38**, 893 (1988)
6. J.M. Tarascan et al., Phys. Rev. **B38,** 8885 (1988)
7. Z.Z. Sheng, A.M. Hermann, Nature **332**, 55 (1988)
8. Z.Z. Sheng, A.M. Hermann, Nature **332**, 138 (1988)
9. R.M. Hazen et al., Phys. Rev. Lett. **60,** 1657 (1988)
10. S.S.P. Parkin et al., Phys. Rev. Lett. **60**, 2539 (1988)
11. S.N. Putilin et al., Mater. Res. Bull. **26,** 1299 (1991)
12. S.S.P. Parkin et al., Phys. Rev. **B38**, 6531 (1988)
13. S.N. Putilin et al., Nature **362**, 226 (1993)
14. S.N. Putilin et al., Physica **C212**, 266 (1993)
15. A. Schlling et al., Nature **363**, 56 (1993)

[1] *Fermi-liquid* characterizes the metallic state with non-interacting quasi-particles. The low-energy excitations (i.e. quasi-particles are in many ways analogous to electrons. Quasi-particles determine the properties at low temperature. The quasi particles are strongly modified (renormalized) by the many electron interactions and by interaction with phonons.

http://www.springer.com/978-3-642-00711-8

High-Temperature Superconductors
Saxena, A.K.
2010, XIV, 223 p. 130 illus., Hardcover
ISBN: 978-3-642-00711-8